BMC Gastroenterology

RESEARCH

Open Access

Expression profile and N6-methyadenosine modification of circular RNA analysis in MAFLD

Mengyao Zheng[1], Dongyun Cun[2], Haiyu He[1], Xuancheng Xie[1], Hongtao Lei[3], Wen Fu[1], Wenlin Tai[4*] and Jinhui Yang[1*]

Abstract

Background To analyze the expression patterns of circRNAs in metabolic associated fatty liver disease (MAFLD) and the regulation of m^{6}A methylation on those circRNAs.

Methods The expression profile of CircRNA in MAFLD and normal control liver tissues was analyzed by microarray. Predict the potential m^{6}A sites of the differentially expression circRNAs (DECs) via the SRAMP website. The biological functions and molecular interactions of DECs were analyzed by GO and KEGG analyses. The selected DECs were verified by MeRIP-qPCR and RT-qPCR.

Results There were 59 DECs in MAFLD liver tissues compared with normal control liver tissues. We found that m^{6}A sites with high or very high confidence were present in 39 of these DECs. Four randomly selected DECs were validated by RT-qPCR, hsa-MLIP_0004, hsa-CHD2_0084 and hsa-FOXP1_0001 matched well with the microarray results. m^{6}A qualification of them were conducted by MeRIP-qPCR, the m^{6}A methylation levels are significantly different between the MAFLD and NC groups.

Conclusion In MAFLD, the dysregulated expression of circRNAs may be influenced by m^{6}A modifications. This study provides preliminary evidence suggesting that m^{6}A-mediated regulation of circRNAs could play a role in the progression of MAFLD, laying the foundation for exploring the epigenetic regulation of circRNAs in MAFLD and offering potential avenues for future diagnostic and therapeutic strategies.

Trial registration Not applicable.

Keywords Circular RNA, MAFLD, m^{6}A modification

*Correspondence:
Wenlin Tai
taiwenlin@kmmu.edu.cn
Jinhui Yang
yangjinhuikyfey@163.com
[1]Department of Gastroenterology, The Second Affiliated Hospital of Kunming Medical University, Kunming, Yunnan 650101, China
[2]Department of Hepatobiliary Surgery, The Second Affiliated Hospital of Kunming Medical University, Kunming, Yunnan 650101, China
[3]Public Health College, Kunming Medical University, Kunming, China
[4]Department of Clinical Laboratory, Yunnan Molecular Diagnostic Center, The Second Affiliated Hospital of Kunming Medical University, Kunming, Yunnan 650101, China

Background

Metabolic associated fatty liver disease (MAFLD) also known as non-alcoholic fatty liver disease (NAFLD), is a common fatty liver disease, that affects around 30% of the global population [1]. Patients with MAFLD are at a high risk of developing intrahepatic complications, such as liver cirrhosis and carcinoma, and they also face a high all-cause mortality rate [2]. Additionally, MAFLD is associated with various extrahepatic diseases, including cardiovascular disease [3], COVID-19 [3], chronic kidney disease (CKD) [4], coeliac disease [5], and thyroid hormones [6]. MAFLD is characterized by liver steatosis accompanied by type 2 diabetes (T2DM), overweight or obesity, and metabolic syndrome (MetS) [7]. Consequently, an unhealthy diet, excessive calorie and fructose intake, and lack of physical exercise are key contributors to this pathological condition. However, interindividual susceptibility to MAFLD can also be influenced by other factors, such as changes in mRNA and non-coding RNAs [8–10], which may become new targets for predicting prognosis, diagnosing disease degree and intervening treatments for MAFLD. Despite its clinical significance, there are limited studies on circRNAs in MAFLD. Therefore, this study aims to explore the expression profile of circRNAs and m^6A in MAFLD, as well as the regulatory relationship between them.

Circular RNAs (circRNAs) are a class of endogenous non-coding RNAs for gene regulating, which form covalently closed continuous circular structures through specific splicing methods [11]. CircRNAs are mainly rooted in the protein-coding exon region of eukaryotes, can regulate gene expression after transcription and are closely related to human tumors, metabolic diseases, liver diseases, etc [12]. In addition, growing evidence suggests that circRNAs play a role in the onset and progression of NAFLD [13–16]. In this study, we compared circRNA expression profiles of MAFLD liver tissue with normal liver tissue using microarray analysis. In eukaryotic mRNA, N6-methyadenosine (m^6A) modification is one of the most plentiful forms, and its function is regulated by three types of methylases, methyltransferases (writers), demethylases (erasers), and the binding proteins (readers) [17]. Recently, a number of studies have revealed that m^6A methylation participates in the onset and progression of diseases by regulating circRNAs [18]. Finding the differentially expressed circRNAs (DECs) and exploring the regulatory relationship between m^6A methylation and circRNAs may provide new directions for the pathogenesis of MAFLD.

Methods

Patient samples

This work got approval of the Research Ethics Committee of the second affiliated Hospital of Kunming Medical University (code: Shen-PJ-2020-26). Liver tissue samples were collected from 11 patients with MAFLD and 11 patients with hepatic hemangioma at the Second Affiliated Hospital of Kunming Medical University between December 2020 and December 2021. The liver tissues from MAFLD patients with liver pathologically confirmed fatty liver (steatosis grade 1–3, fibrosis grade 1–2) were assigned to the MAFLD group, while the normal liver tissues adjacent to hemangioma were used as the normal control group (Fig. 1, Supplementary1). The resected liver tissue samples were immediately frozen in liquid nitrogen at -80℃ for subsequent detection. Five pairs of samples were sequenced by microarray analysis of circular RNA(Table 1), and six pairs of samples were validated by RT-qPCR and MeRIP-qPCR.

RNA extraction & sequencing

Total RNA was extracted using TRIzol (Invitrogen, CA, USA), then the magnetic beads coated with streptavidin were combined with the probe and rRNA complex

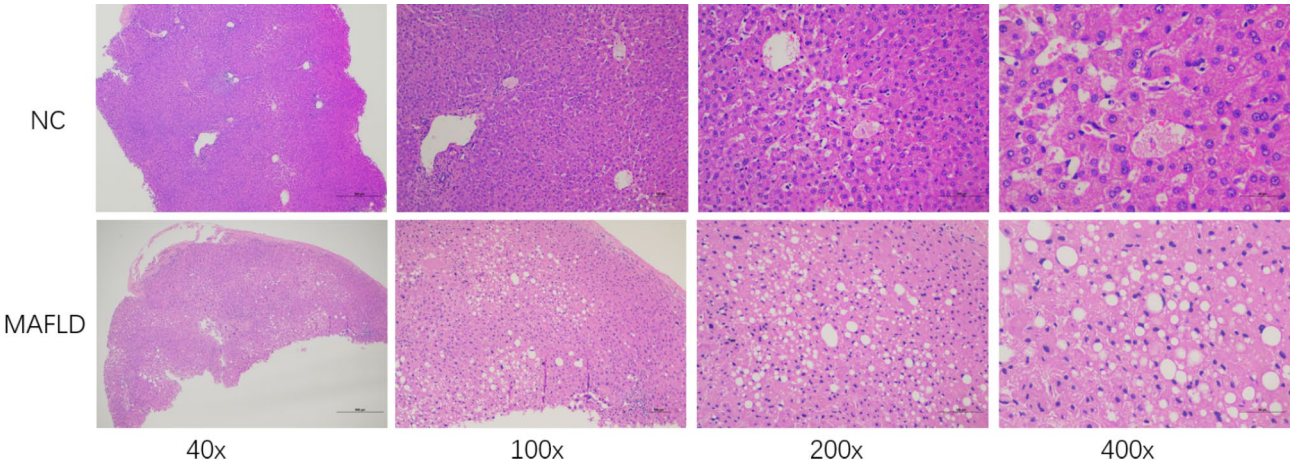

Fig. 1 Liver tissues of normal control group (NC) and metabolic-associated fatty liver disease group (MAFLD) were stained with HE

Table 1 Clinical characteristics of the patients

Characteristics	MAFLD($n=5$)	NC($n=5$)	*p*-value
Age(years, mean)	55.2 ± 10.96	56.4 ± 13.94	0.883
Gender(male/female)	5/0	5/0	
BMI(kg/m2,mean)	29.17 ± 1.15	20.84 ± 1.62	0.000
SBP(mmHg, mean)	137 ± 17.25	113 ± 11.59	0.036
DBP(mmHg, mean)	77.6 ± 8.62	71.2 ± 8.79	0.278
Triglycerides(mmol/L, mean)	3.75 ± 4.04	1.05 ± 0.35	0.039
HDL(mmol/L, mean)	1.21 ± 0.15	1.19 ± 0.36	0.893
Glucose(mg/dL, mean)	8.85 ± 3.63	5.2 ± 0.19	0.055
ALT(U/L, mean)	88.8 ± 21.72	28.46 ± 13.2	0.001
AST(U/L, mean)	50.2 ± 9.63	28.64 ± 4.67	0.002
Uric acid(umol/L, mean)	408.8 ± 64.1	310.6 ± 88.47	0.079

to deplete ribosomal RNA, purify and fragment RNA. Then the fragmented RNA was added to the pre-mixed Dynabeads Protein A magnetic beads and antibodies, incubated at 4 °C for 2 h to bind the m^6A methylated RNA fragment to the antibody. The RNA fragments that were non-specifically bound to the magnetic beads were removed, and eluents containing m^6A were added to competitively eluate the RNA fragments that were specifically bound and modified with m^6A and labeled as IP. Using IP and Input RNA as templates. The first-strand cDNA was synthesized by the SuperScript IV reverse transcription kit, which was the template to synthesize the second-strand cDNA containing dUTP. Added the adenine to the 3 'end, and T4 DNA ligase connects both ends of sequencing splicing and cDNA. The cDNA library was purified and screened by the DNA purification magnetic bead II nucleic acid fragment screening kit, at last the cDNA library was amplified by PCR, Qubits were used to precisely quantify library concentration. The Agilent 2100 bioanalyzer measured the size distribution of the constructed library fragments, and Illumina high-throughput sequencing platform was used to detect the library with 2 × 150 bp double-ended sequencing strategy.

CircRNA microarray analysis

FastQC software and R software were used to assess the quality of sequencing data. The analysis involved removing adapter sequences and trimming low-quality bases. Specifically, sequences with a Phred quality score below 15 ($Q < 15$) were filtered out, and reads shorter than 40 base pairs were excluded. After quality control, reads were aligned to the reference genome using HISAT2 software with default parameters, allowing up to two mismatches per read. Alignment results were statistically analyzed using Picard tools, which provided metrics such as alignment rates, duplication levels, and insert size distributions to ensure data quality. Reads that did not map to the reference genome were extracted and processed further using CIRI2 software, which employed a robust algorithm to identify back-splice junctions, predict the starting and ending locations of circRNAs, annotate their origin genes, and quantify their expression levels across samples. To determine differentially expressed circRNAs (DECs) between the MAFLD and NC groups, DESeq2 software was utilized with the following criteria:|log2 fold change| > 2 and adjusted p-value < 0.05. The DESeq2 analysis included normalization of read counts using the median-of-ratios method to account for differences in sequencing depth and RNA composition across samples. Volcano plots and heatmaps were generated to visualize the DECs, highlighting significant upregulation and downregulation patterns in circRNA expression.

SRAMP analysis

The SRAMP website (www.cuilab.cn/sramp/) was used to predict potential m6A sites on circRNAs [19]. The RNA sequences were analyzed using the mature generic predictive model, which evaluates sequence-derived features and secondary structures. The confidence levels of m^6A site predictions were categorized into four groups: low, moderate, high, and very high. For this study, m^6A sites with high or very high confidence were considered significant. The analysis parameters were kept at default settings, as recommended by the SRAMP tool documentation.

Data analysis

Gene ontolology (GO) and Kyoto Encyclopedia of Genes and Genomes (KEGG) enrichment analysis of DECs was performed using R-package clusterProfiler. For all experiments, one representative experimental data was selected from triplicate data. Data were expressed as mean ± standard deviation (S.D.), and then evaluate whether the difference was statimstically significant by t test. All data were statistically analyzed and visualized using R or GraphPad Prism(verson 8.0), and the statistical significance of the difference was defined as $P < 0.05$.

RT-qPCR

DECs expression level was detected by real-time quantitative PCR (RT-qPCR) using SYBR® Premix Ex Taq™ II(Tli RNaseH Plus). ROX dye was added to correct the interpore signal. There were 3 multiple pores at each site. The internal reference primer β-actin was added; The optimized procedure was used for amplification on the ABI 7900 fluorescence quantitative PCR apparatus, and the melting curve program was added. After the reaction, the amplification and melting curves of reference and target genes in each sample of Real-Time PCR were confirmed. The reaction conditions were 95 ° C for 30 s, 95 ° C for 5 s, and 60 ° C for 30 s for 40 cycles. The final Ct value of each detected gene was the average of the Ct values of the three complex pores, and the target gene

was quantitatively quantified by ΔCt method. The relative expression of target gene = 2-ΔCt。 .

MeRIP-qPCR

For m^6A modification site-specific detection, primers targeting the modified sites were designed and used for fluorescence quantitative PCR (qPCR). The SYBR Green fluorescent dye was employed to detect amplification, and ROX dye was included as an internal reference to correct for variations in fluorescence signal between different wells. Three technical replicates were performed for each target site to ensure data reliability. The PCR amplification was conducted using an ABI 7900 fluorescence quantitative PCR system with a two-step amplification protocol. The reaction conditions included an initial denaturation step, followed by a series of amplification cycles, with a final melting curve analysis to confirm the specificity of the PCR products. The melting curve program was implemented to ensure that the observed fluorescence signals were attributable to specific amplification products. After amplification, the resulting amplification curves and melting curves for each sample were analyzed to verify the efficiency and specificity of the reaction. The average cycle threshold (Ct) values from the three technical replicates were calculated and used as the final Ct value for each sample. The percentage of input (%Input) for each target site was calculated using the following formula: $\%Input = 2^{-[Ct_{IP} - (Ct_{Input} - Log2\ 10)]}$.

Results

We performed circRNA microarray on five MAFLD liver tissues and five normal control (NC) liver tissues. The expression density distribution of circRNAs in the MAFLD group and NC group was exhibited, the concentration of gene expression in the whole sample was between 0 and 2 (Fig. 2A). We found 59 circrnas with significant differences ($log2FC > 2$ and $p < 0.05$) in expression levels between MAFLD and NC group, and then hierarchical clustering analysis (heatmap) showed the distribution of differentially expressed circRNAs (DECs) (Fig. 2B), scatter plots assessed the changes in circRNA expression profiles (Fig. 2C). Among the 59 DECs, 35 circRNAs were up-regulated and 24 circRNAs were down-regulated, of which the top ten up-regulated and down-regulated circRNAs with the highest fold change value are shown in Tables 2 and 3. Principal component analysis(PCA) was applied to analyze the difference of DECs clustering. The results showed that the first and second principal components accounted for 50.944% and 10.409% of the total transcriptome variables, respectively, completely differentiates the MAFLD group from the normal control group, and it proves that the circRNAs expression levels of the two groups are significantly different (Fig. 2D). Statistically significant DECs between the two groups are shown with the use of M-A plots (Fig. 2E).

Analysis of m6A modification of DECs

N6-methylladenosine (m^6A) is a common internal component of both mRNA and non-coding RNA (ncRNAs) that is widely present in eukaryotes, accounting for about 50% of the total methyl-labeled ribonucleoside [20]. The SRAMP website tool was used to predict the potential m6A site of DECs, and the potential role of m^6A modification on circRNA modification of MAFLD was explored [19]. Of the 59 DECs, 50 DECs had m^6A sites, of which 26 upregulated circrnas and 13 downregulated circrnas had high or very high confident m^6A sites (Fig. 3A). Figure 3B shows the results of hierarchical clustering of m6A-DECs in the MAFLD and NC groups by a heat map, and a scatter plot visualizes the distribution of m6A-DECs (Fig. 3C).

GO & KEGG pathway analysis

Annotate the functions of host genes in m6A-DECs by Gene ontology (GO) analysis to explore the potential functions of m6A-DECs. Figure 3D shows three enriched GO terms, biological process (BP), cellular component (CC), and molecular function (MF) related, respectively. The most significant GO terms that we found to be associated with biological processes were activation of immune response, regulation of monocyte differentiation and muscle hypertrophy. The most significant cellular components were blood microparticle, vesicle membrane, immunoglobulin complex and low-density lipoprotein particle. The most significant molecular function were hydro-lyase activity, ribosome binding, carbon-oxygen lyase activity, structural constituent of cytoskeleton (Fig. 3D). Kyoto Encyclopedia of Genes and Genomes (KEGG) pathway analysis was used to further explore the biological functions and molecular interactions of these m6A-DECs. The top ten enriched KEGG pathways, including toxoplasmosis, influenza A, tryptophan metabolism, and fatty acid degradation pathways, suggesting the potential role of m6A-DECs in MAFLD (Fig. 3E).

Analysis of m^6A methyltransferases of m^6A-DECs

Three classes of methylases, m^6A methyltransferases (m^6A writers), m^6A demethylases (m^6A erasers), and m^6A-binding proteins (m^6A readers) work together to modify m6A [20]. Thus, we sought to identify m^6A-DECs which can bind m^6A methyltransferases with the use of the circAtlas v2.0 database. RBPs were obtained from this database, m^6A methylases were selected from those RBPs. In total, 35 m^6A-DECs can bind 12 potential m^6A methyltransferases. twelve potential m^6A methyltransferases include two m^6A writers: RBM15 and RBM15B; one

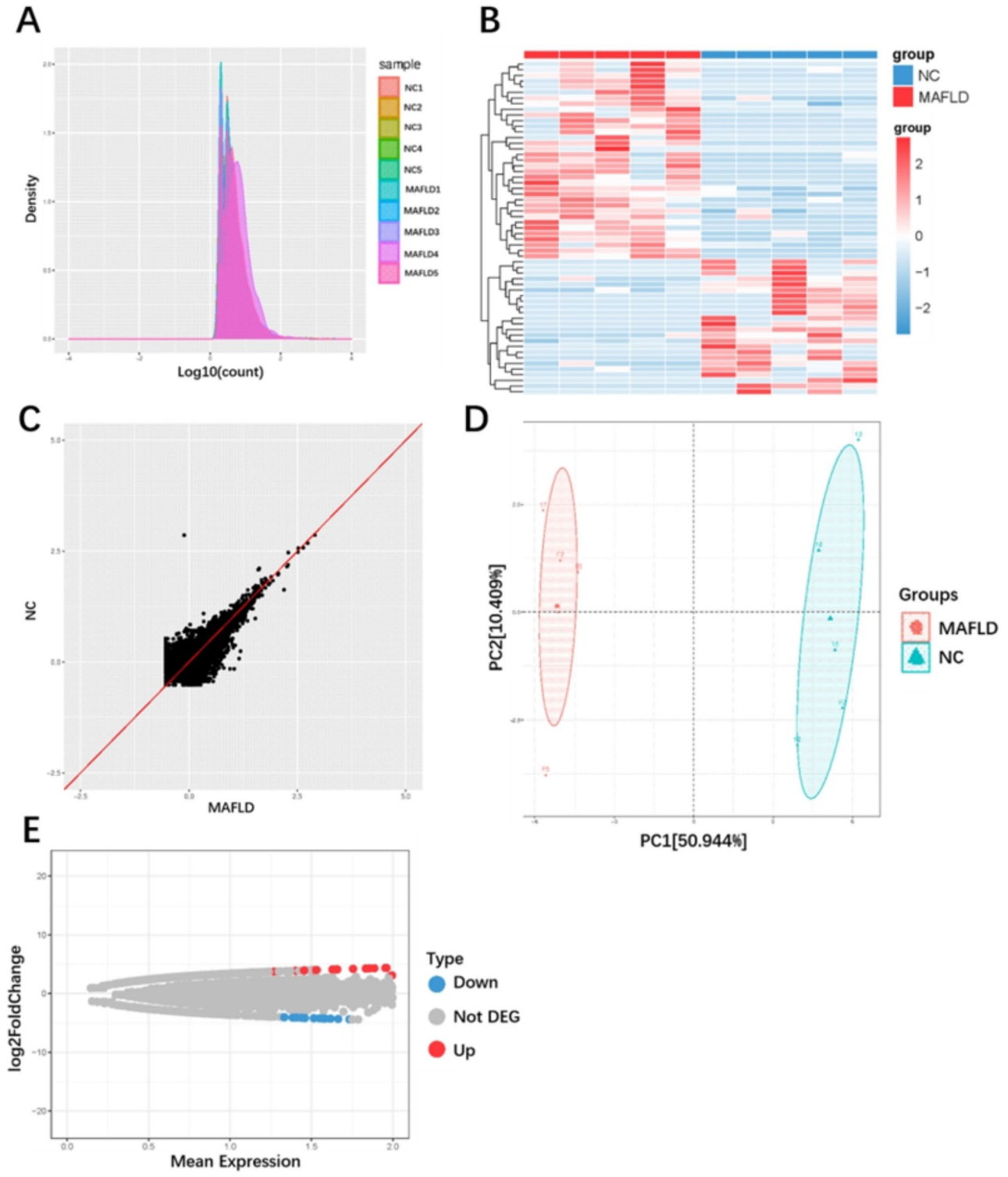

Fig. 2 Analysis of differentiated expressed circular RNAs(DECs) in MAFLD liver tissues and normal liver tissues. (**A**) Expression density distribution of all circRNAs among the MAFLD group and normal control group. The horizontal coordinate is the expression amount of circRNA, the vertical coordinate is the density of circRNA, each color represents a sample, the sum of all probabilities is 1, and the region with the most concentrated gene expression amount of all samples is between 0 and 2. (**B**) Hierarchical cluster analysis (heat map) shows the distribution of DECs between MAFLD and NC groups. (**C**) Scatter plot assesses the distribution of the DECs between MAFLD and NC groups. (**D**) Principal component analysis(PCA)was used to analyze the difference of DECs clustering between MAFLD and NC groups. (**E**) M-A scatter plot shows the distribution of DECs between the two groups. The vertical M value is log2(FC), and the horizontal A value is Mean expression

Table 2 Top ten upregulated circrnas

Circatlas ID	*p*-value	Log2FC	Gene name
hsa-ADH1B_0017	2.45691E-13	22.16394429	ADH1B
hsa-IGHA1_0001	1.52137E-07	6.55999671	IGHA1
hsa-HLA-DRB1_0005	0.049744728	5.948135076	HLA-DRB1
hsa-intergenic_000786	9.15861E-05	5.17881624	intergenic
hsa-GTF2IP7_0003	0.008245411	4.354361427	GTF2IP7
hsa-ATXN10_0026	0.017309747	4.353595925	ATXN10
hsa-CASC4_0009	0.005898836	4.295555412	CASC4
hsa-KPNA5_0009	0.010824136	4.288708581	KPNA5
hsa-RPN2_0008	0.021522777	4.259509943	RPN2
hsa-PARN_0021	0.007800024	4.195948979	PARN

Table 3 Top ten downregulated circrnas

Circatlas ID	*p*-value	Log2FC	Gene name
hsa-ORM2_0001	0.000405151	-9.8526312	ORM2
hsa-MYO10_0008	0.002138364	-4.86004512	MYO10
hsa-LRBA_0030	0.006063396	-4.81037946	LRBA
hsa-BIRC6_0078	0.020823216	-4.38775307	BIRC6
hsa-AFF4_0005	0.013707547	-4.32959909	AFF4
hsa-ADAMTS13_0001	0.025830838	-4.28349474	ADAMTS13
hsa-C9orf84_0005	0.044127322	-4.26740731	C9orf84
hsa-SLC1A1_0010	0.02971349	-4.23515232	SLC1A1
hsa-EHHADH_0003	0.030657889	-4.21841618	EHHADH
hsa-PTPRM_0044	0.034558593	-4.17415822	PTPRM

m^6A eraser: FTO; nine m^6A readers: IGF2BP1, IGF2BP2, IGF2BP3, HNRNPC, HNRNPA2B1, YTHDC1, YTHDF1, YTHDF2, YTHDF3 (Fig. 4A). hsa-CDYL_0005 can bind ten m^6A methyltransferases, include m^6A writers and readers. However, how these m^6A methyltransferases regulate circRNAs and whether they bind by m^6A sites needs to be further verified.

RT-qPCR for validation of circrna expression

To verify the sequencing results, two upregulated circRNAs (hsa-MLIP_0004 and hsa-CHD2_0084) and two down-regulated circRNA (hsa-FOXP1_0001 and hsa-HAAO_0002) were randomly selected and RT-qPCR was performed in 6 MAFLD liver tissues and 6 normal control liver tissues (Supplementary 2). The results indicated that among the four DECs, hsa-MLIP_0004 and hsa-CHD2_0084 were also up-regulated in MAFLD, while hsa-FOXP1_0001 was down-regulated in MAFLD, consistent with the sequencing results (Fig. 4B). hsa-HAAO_0002 expression was upregulated in MAFLD liver tissue, which was in contrast to the sequencing results ($P = 0.24$) (Fig. 4B).

m6A modification level of circrnas by MeRIP-qPCR

We performed MeRIP-qPCR to detect the m^6A methylated level of two upregulated circRNAs (hsa-MLIP_0004 and hsa-CHD2_0084) and one down-regulated circRNA (hsa-FOXP1_0001) (Supplementary 3, 4). The results indicated that the m^6A methylation levels of hsa-CHD2_0084 and hsa-FOXP1_0001 were upregulated in the MAFLD group, and the m^6A methylation levels of hsa-MLIP_0004 was down-regulated in the MAFLD group (Fig. 4C).

Discussion

CircRNAs are a class of closed loop endogenous RNAs, which is involved in the onset and progression of many diseases and may be a kind of potential new biomarker [21]. In NAFLD, previous studies have confirmed that circ0046366, circ0046367, and circScd1 mediate fat deposition in hepatocytes by regulating signal transduction pathways [12–14];circRNA SCAR is closely related to the progression of lipid degeneration in NAFLD [15]; upregulation of circRNA_0001805 promotes the release of glycyrrheic acid, thereby reducing the lipid accumulation in liver tissue and acting synergistically on NAFLD-induced lipid metabolism disorders [16]. MAFLD, in contrast to NAFLD, offers a more expansive and inclusive perspective [7]. It considers not just the buildup of fat, but also various metabolic factors like obesity, type 2 diabetes, high cholesterol, and hypertension. Hence, the circRNA expression pattern in MAFLD might diverge from that observed in NAFLD, suggesting potentially distinct roles for circRNA in MAFLD pathogenesis. Nonetheless, research on circRNA in MAFLD liver tissues is scarce, leaving our knowledge of DECs and their functions in MAFLD relatively limited.

In this study, we compared the expression profiles of circRNA in MAFLD and NC tissues by circRNA sequencing. The results showed 35 upregulated circRNAs and 24 downregulated circRNAs in MAFLD. The PCA result showed that it completely differentiates the MAFLD group from the normal control group. That means circRNA may play an important role in MAFLD. To confirm the microarray data, four dysregulated circRNAs were selected for RT-qPCR validation, which of the three circRNAs expression level had the same trend as the sequencing results. These findings indicate that these differentially expressed genes (DEGs) might contribute to the onset and progression of MAFLD, further investigation into their mechanisms could uncover novel insights into diagnosing and treating MAFLD. The mechanistic role of hsa-FOXP1_0001 remains unexplored in MAFLD; however, two studies have investigated its function in other pathological conditions; hsa-FOXP1_0001 (hsa_circ_0008234) is highly expressed in cutaneous squamous cell carcinoma(cSCC) tissues and promotes the proliferation of cSCC by targeting miR-127-5p to regulate the expression of ADCY7 [22]; hsa-FOXP1_0001 was up-regulated in colon cancer tissues and increased the proliferation, invasion and migration of colon cancer through miR-338-3p/ETS1/PI3K/AKT axis [23]. Studies

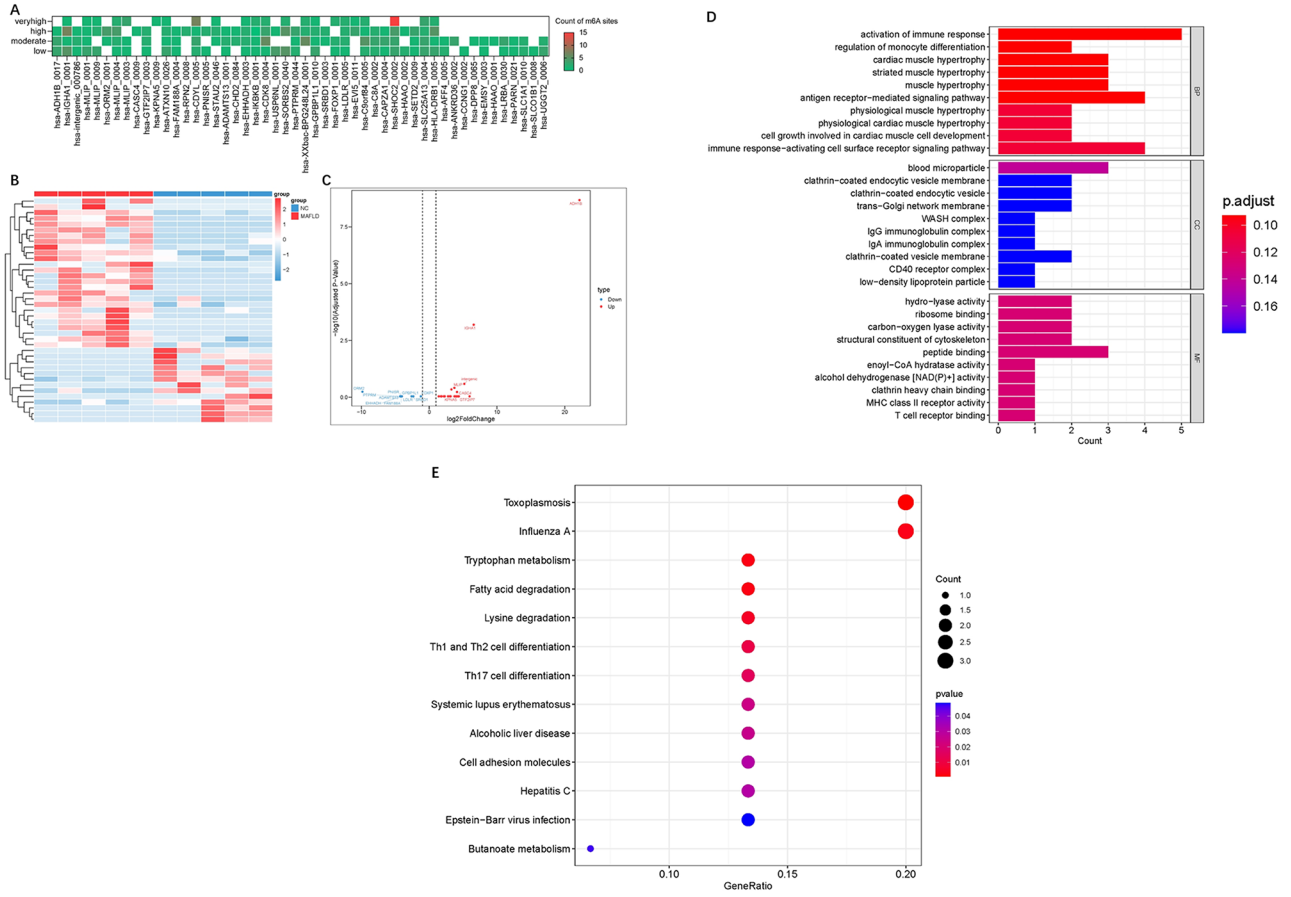

Fig. 3 Analysis of differentiated expressed circular RNAs (DECs) with high or very high confident m^{6}A methylated sites (m^{6}A-DECs) in MAFLD liver tissues and NC liver tissues. (**A**) Hierarchical cluster analysis (heat map) shows the m^{6}A methylated sites of DECs, the m^{6}A methylated sites are divided into four types: very high, high, moderate and low confidence (**B**) Hierarchical cluster analysis (heat map) of microarray data assessed the significant expression of m^{6}A-DECs between MAFLD and NC groups. (**C**) Scatter plot represents the default significant fold change. (**D**) The GO analysis categorized the m^{6}A-DECs into different groups under the theme of biological process (BP), cellular component (CC) and molecular function (MF). (**E**) Kyoto Encyclopedia of Genes of analysis of m^{6}A-DECs

pertaining to hsa-MLIP_0004 are limited, with only one investigation employing next-generation sequencing analysis of human and murine heart failure samples; this study identified differentially expressed circ-MLIP, confirming its circular nature and delineating reverse-spliced exons, yet further functional exploration was not pursued [24]. Currently, there is no research on hsa-CHD2_0084, but its source gene Chromodomain Helicase DNA Binding Protein 2 (CHD2) has been studied. Researchers have utilized the Gene Expression Omnibus (GEO) database to identify differentially expressed transcription factors from liver tissue chip data of 26 healthy volunteers and 109 NAFLD patients, including CHD2 [25]; another study demonstrated the association of CHD2 with type 2 diabetes in both mice and humans, suggesting its potential role as an obesity gene [26]. The above study suggests that CHD2 may be involved in the occurrence and development of MAFLD, further exploration of the role of hsa-CHD2_0084 in MAFLD may yield promising results.

N6-methyladenosine is the abundantly RNA modifications, and these modifications are present on mRNA, lncRNA, and circRNA. It has been revealed in several studies that, m^{6}A may affect all stages of the disease by regulating circRNA. m^{6}A methylation can regulate circNSUN2 to promote cytoplasmic output and stabilize HMGA2 to promote the process of colorectal cancer liver metastasis [27]; IFN-regulator-1 regulates the expression level of circ0029589 through m^{6}A modification to induce macrophage dysfunction in acute coronary syndrome patients [28]; m^{6}A methylation also regulates circRNA immunity and metabolism [29, 30]. In this study, we described the m^{6}A sites of DECs in MAFLD and the NC liver tissues. We found that among 59 DECs, there were high or very high confident m^{6}A sites in 39 circRNAs. In conclusion, our findings suggest that m^{6}A modifications in DECs is commonly exited in human liver tissue and closely associated to the function of circRNA, providing a

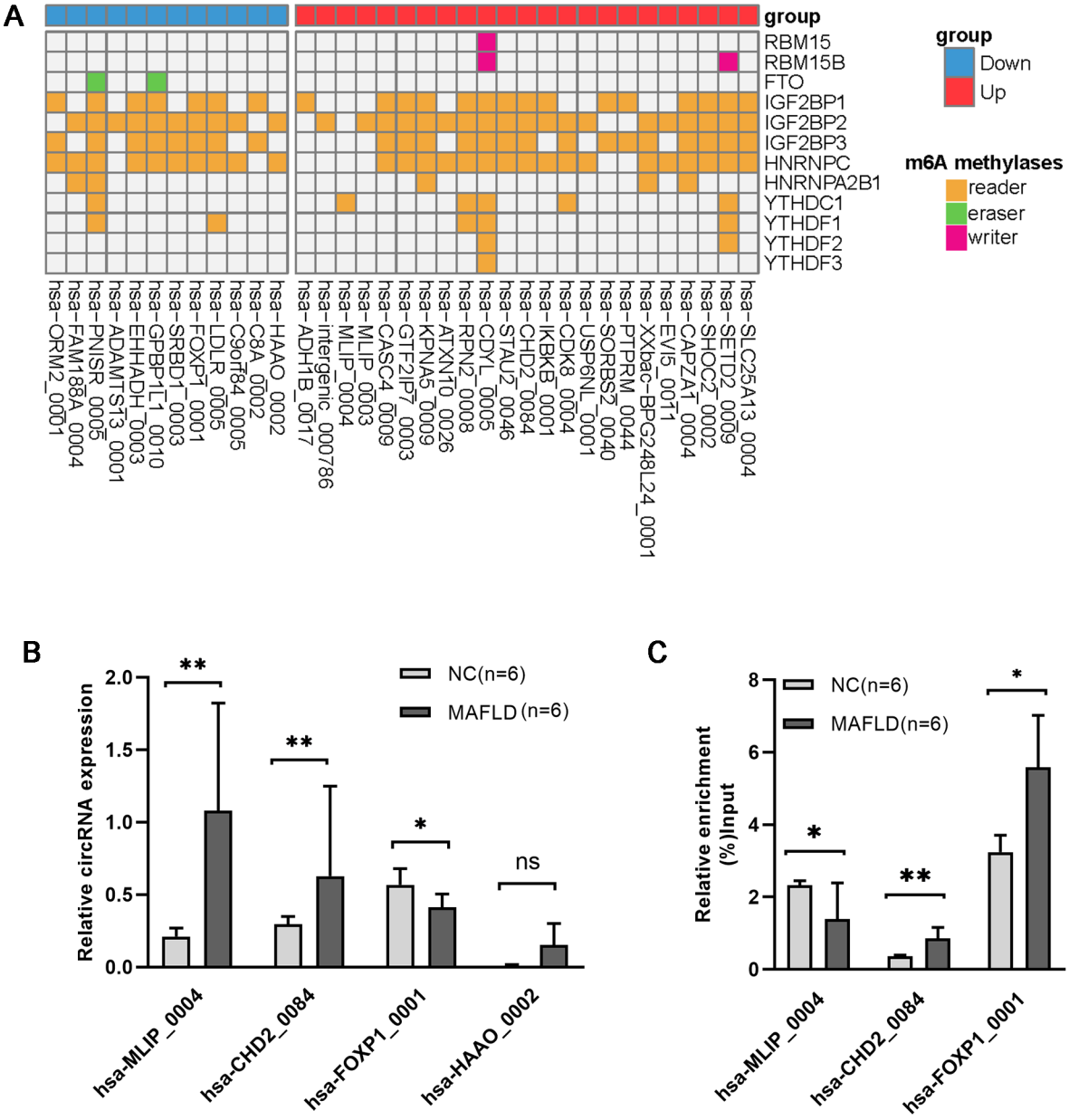

Fig. 4 (**A**) Hierarchical cluster analysis (heat map) shows the binding m^{6}A methylases of m^{6}A-DECS. (**B**) Relative expression of hsa-MLIP_0004, hsa-CHD2_0084, hsa-FOXP1_0001 and hsa-HAAO_0002 in 6 normal human liver (NC) tissues and 6 MAFLD human liver tissues quantified by RT-qPCR. (**C**) m6A methylated level of hsa-MLIP_0004, hsa-CHD2_0084 and hsa-FOXP1_0001 in 6 normal human liver (NC) tissuesand 6 MAFLD human liver tissues quantified by MeRIP-qPCR; *$P < 0.05$, **$P < 0.01$

new direction for the pathogenesis and therapeutic directions of MAFLD.

The potential role of m6A-DECs was predicted by GO and KEGG analysis. We found one of the enriched pathways was directly related to low-density lipoprotein particle in MAFLD. The biological functions and molecular interactions of these m6A-DECs host genes were further investigated by analysis of KEGG pathway, fatty acid degradation pathway may related to the development of MAFLD. Together, these results suggest that those m6A-DECs may have a potential affection in the progression of MAFLD. To confirm the predicted results, two upregulated m^{6}A-DECs and one downregulated m^{6}A-DECs were selected and further verified in MAFLD and normal

control liver tissues by MeRIP-qPCR. We found that the m^{6}A methylation levels of these three circRNAs were significantly different between the two groups. Interestingly, the expression levels of hsa-CHD2_0084 are consistent with the trend of m^{6}A methylation levels, whereas the expression levels of hsa-FOXP1_0001 and hsa-MLIP_0004 exhibit an opposite trend to the m^{6}A methylation levels. All the three circRNAs can bind to m^{6}A methyltransferases, and the m^{6}A methyltransferases they bind are "readers", including IGF2BP1, IF2BP2, IGF2BP3, HNRNPC, YTHDC1, and YTHDF1. The IGF2BP family (including IGF2BP1, IGF2BP2, and IGF2BP3) recognizes m^{6}A-modified sites on circRNAs to enhance their stability by preventing degradation through ribonucleases, thereby extending their half-life. Some circRNAs possess translational potential, and the IGF2BP family facilitates translation by binding to m^{6}A sites, ultimately influencing protein production. HNRNPC (Heterogeneous Nuclear Ribonucleoprotein C) is another m^{6}A "reader" protein that modulates RNA splicing and secondary structure. The m^{6}A modification induces changes in RNA secondary structure (known as the "m^{6}A switch"), making it easier for HNRNPC to bind to target RNAs. This interaction affects the biogenesis of circRNAs by influencing the selection of circularization sites and, consequently, the diversity and abundance of circRNAs.

YTHDC1, a nuclear m^{6}A "reader" protein, primarily regulates RNA nuclear export, splicing, and degradation. By binding to m^{6}A-modified circRNAs, YTHDC1 facilitates their export from the nucleus to the cytoplasm. It can also indirectly influence circRNA splicing or circularization by modulating the availability of m^{6}A sites. YTHDF1, a cytoplasmic m^{6}A "reader" protein, plays a critical role in enhancing the translation of m^{6}A-modified RNAs. It binds to m^{6}A-modified circRNAs and promotes ribosome recruitment, thereby increasing the translation efficiency of circRNAs. These enzymes influence circRNA function by affecting their stability, splicing, nuclear export, and translation, highlighting their role in disease mechanisms [31, 32].

Despite the valuable insights provided by this study, several limitations should be acknowledged. First, the relatively small sample size (five cases per group for microarray analysis and six for validation) may limit the generalizability and statistical power of our findings. Future studies with larger cohorts and diverse clinical samples are needed to confirm these preliminary results and enhance their applicability. Second, the current study primarily focused on identifying correlations between m^{6}A modifications and circRNA expression in MAFLD without exploring causative mechanisms. While we observed significant differences in m^{6}A methylation levels and circRNA expression, functional experiments, such as knockdown or overexpression of m^{6}A regulatory enzymes (e.g., IGF2BPs or HNRNPC) and circRNAs, are necessary to elucidate the precise molecular mechanisms underlying these associations. Third, the exploratory nature of the study limits the depth of mechanistic validation, such as the role of m^{6}A-modified circRNAs in MAFLD-related pathways like lipid metabolism or inflammation. These aspects warrant further investigation to uncover the biological relevance of m^{6}A-modified circRNAs in MAFLD pathogenesis. These limitations reflect the exploratory stage of this research and highlight the need for more comprehensive studies to validate and expand on these findings.

This study provides preliminary evidence that the dysregulation of circRNA expression in MAFLD liver tissues may be influenced by m6A modifications. By integrating circRNA expression profiling and m^{6}A site prediction, we identified specific m^{6}A-modified circRNAs with altered expression levels in MAFLD, shedding light on the potential regulatory role of m6A in circRNA-mediated pathogenesis.

Although exploratory, these findings offer new perspectives on the role of m^{6}A-modified circRNAs in MAFLD and provide a foundation for future research aimed at elucidating their functional and mechanistic significance. Further investigations into the biological functions and molecular pathways of m^{6}A-modified circRNAs could lead to novel insights into the pathogenesis of MAFLD and identify potential therapeutic targets for its treatment.

Conclusion

This study identified differentially expressed circRNAs in MAFLD and NC liver tissues, including hsa-MLIP_0004, hsa-CHD2_0084, and hsa-FOXP1_0001, which were found to have m^{6}A binding sites with altered methylation levels. These findings suggest a potential regulatory role of m^{6}A methyltransferases in modulating circRNA expression in MAFLD.

Although this study provides preliminary evidence of the involvement of m^{6}A-mediated circRNA regulation in MAFLD, further investigation is needed to validate these associations and establish causative mechanisms. Future research should focus on functional studies to elucidate the biological roles of m^{6}A-modified circRNAs in MAFLD progression. This work lays a foundation for deeper insights into the epigenetic regulation of circRNAs in metabolic liver diseases and highlights potential avenues for further exploration.

Abbreviations

MAFLD	Metabolic associated fatty liver disease
DECs	Ifferentially expression circRNAs
NAFLD	Non-alcoholic fatty liver disease
CKD	Chronic kidney disease
T2DM	Type 2 diabetes
MetS	Metabolic syndrome

circRNAs	Circular RNAs
NC	Normal control
DECs	Differentially expressed circRNAs
PCA	Principal component analysis
GO	Gene ontology
BP	Biological process
CC	Cellular component
MF	Molecular function
KEGG	Kyoto Encyclopedia of Genes and Genomes

Supplementary Information

The online version contains supplementary material available at https://doi.org/10.1186/s12876-025-03722-4 .

Supplementary Material 1

Acknowledgements
Not applicable.

Author contributions
MYZ, DYC and HYH carried out the studies, participated in collecting data, and drafted the manuscript. XCX performed the PCR, HTL and WF performed the statistical analysis and participated in its design. TWL and JHY participated in acquisition, analysis, or interpretation of data and draft the manuscript. All authors read and approved the final manuscript.

Funding
This work was supported by the National Natural Science Foundation of China (81760383, 82160106); Yunnan Provincial Science and Technology Department-Kunming Medical University Joint Special Key Project (2018FE001(-007)).

Data availability
All data generated or analysed during this study are included in this published article and its supplementary information file.

Declarations

Ethics approval and consent to participate
This work got approval of the Research Ethics Committee of the second affiliated Hospital of Kunming Medical University (code: Shen-PJ-2020-26).

Consent for publication
Not applicable.

Competing interests
The authors declare no competing interests.

Received: 7 March 2024 / Accepted: 21 February 2025
Published online: 11 March 2025

References

1. Meroni M, Longo M, Fracanzani AL, Dongiovanni P. MBOAT7 down-regulation by genetic and environmental factors predisposes to MAFLD[J]. EBioMedicine. 2020;57:102866.
2. Kaya E, Yilmaz Y. Metabolic-associated fatty liver disease (MAFLD): A Multisystemic disease beyond the liver[J]. J Clin Transl Hepatol. 2022;10(2):329–38.
3. Zhou YJ, Zheng KI, Wang XB, Sun QF, Pan KH, et al. Metabolic-associated fatty liver disease is associated with severity of COVID-19[J]. Liver Int. 2020;40(9):2160–3.
4. Sun DQ, Jin Y, Wang TY, Zheng KI, Rios RS, et al. MAFLD and risk of CKD[J]. Metabolism. 2020;115:154433.
5. Rispo A, Imperatore N, Guarino M, Tortora R, Alisi A et al. Metabolic-associated fatty liver disease (MAFLD) in coeliac disease. Liver Int, 2021 Apr;41(4):788-798.
6. Zhang X, Li R, Chen Y, Dai Y, Chen L et al. The role of thyroid hormones and autoantibodies in metabolic dysfunction associated fatty liver disease: TgAb May be a potential protective Factor[J]. Front Endocrinol, 2020Dec 8;11:598836.
7. Lin S, Huang J, Wang M, Kumar R, Liu Y, et al. Comparison of MAFLD and NAFLD diagnostic criteria in real world[J]. Liver Int. 2020;40(9):2082–9.
8. Merve Bayram H, Eren F, Esra Gunes F. The relationship between polyphenols and MiRNAs: A novel therapeutic strategy for metabolic associated fatty liver disease[J]. Hepatol Forum. 2021;2(3):128–36.
9. López-Sánchez GN, Montalvo-Javé E, Domínguez-Perez M, Antuna-Puente B, Beltrán-Anaya FO, et al. Hepatic mir-122-3p, mir-140-5p and mir-148b-5p expressions are correlated with cytokeratin-18 serum levels in MAFLD[J]. Ann Hepatol. 2022;27(6):100756.
10. Sun B, Zhang Y, Zhang M, Liu R, Yang W. Gene therapy targeting miR–212–3p exerts therapeutic effects on MAFLD similar to those of exercise[J]. Int J Mol Med, 2023, 51(2).
11. Jin X, Feng CY, Xiang Z, Chen YP, Li YM. CircRNA expression pattern and circRNA-miRNA-mRNA network in the pathogenesis of nonalcoholic steatohepatitis[J]. Oncotarget. 2016;7(41):66455–67.
12. Li P, Shan K, Liu Y, Zhang Y, Xu L, et al. CircScd1 promotes fatty liver disease via the Janus kinase 2/signal transducer and activator of transcription 5 Pathway[J]. Dig Dis Sci. 2019;64(1):113–22.
13. Guo XY, Sun F, Chen JN, Wang YQ, Pan Q, et al. circRNA_0046366 inhibits hepatocellular steatosis by normalization of PPAR signaling[J]. World J Gastroenterol. 2018;24(3):323–37.
14. Guo XY, Chen JN, Sun F, Wang YQ, Pan Q et al. circRNA_0046367 Prevents Hepatoxicity of Lipid Peroxidation: An Inhibitory Role against Hepatic Steatosis[J]. Oxidative medicine and cellular longevity, 2017, 2017: 3960197.
15. Zhao Q, Liu J, Deng H, Ma R, Liao JY, et al. Targeting Mitochondria-Located circrna SCAR alleviates NASH via reducing mROS. Output[J] Cell. 2020;183(1):76–e9322.
16. Li J, Qi J, Tang Y, Liu H, Zhou K, et al. A nanodrug system overexpressed CircRNA_0001805 alleviates nonalcoholic fatty liver disease via miR-106a-5p/miR-320a and ABCA1/CPT1 axis[J]. J Nanobiotechnol. 2021;19(1):363.
17. Dorn LE, Lasman L, Chen J, Xu X, Hund TJ, et al. The N(6)-Methyladenosine mRNA Methylase METTL3 controls cardiac homeostasis and Hypertrophy[J]. Circulation. 2019;139(4):533–45.
18. Di Timoteo G, Dattilo D, Centron-Broco A, Colantoni A, Guarnacci M, et al. Modulation of circrna metabolism by m(6)A Modification[J]. Cell Rep. 2020;31(6):107641.
19. Zhou Y, Zeng P, Li YH, Zhang Z, Cui Q. SRAMP: prediction of mammalian N6-methyladenosine (m6A) sites based on sequence-derived features[J]. Nucleic Acids Res. 2016;44(10):e91.
20. Chen Y, Lin Y, Shu Y, He J, Gao W. Interaction between N(6)-methyladenosine (m(6)A) modification and noncoding RNAs in cancer[J]. Mol Cancer. 2020;19(1):94.
21. Huang ZK, Yao FY, Xu JQ, Deng Z, Su RG et al. Microarray expression profile of circular RNAs in peripheral blood mononuclear cells from active tuberculosis Patients[J]. Cellular physiology and biochemistry: international journal of experimental cellular physiology, biochemistry, and Pharmacology, 2018, 45(3): 1230–40.
22. Cai L, Wang Y, Wu J, Wu G. Hsa_circ_0008234 facilitates proliferation of cutaneous squamous cell carcinoma through targeting miR-127-5p to regulate ADCY7[J]. Arch Dermatol Res. 2022;314(6):541–51.
23. Wu D, Li Y, Xu A, Tang W, Yu B. CircRNA RNA Hsa_circ_0008234 promotes Colon cancer progression by regulating the miR-338-3p/ETS1 Axis and PI3K/AKT/mTOR Signaling[J]. Cancers (Basel), 2023, 15(7).
24. Huang Z, Zeng Z, Li J, Cai R, He W, et al. [High expression of Circ-PALLD in heart failure is transcriptionally regulated by the transcription factor GATA4][J]. Nan Fang Yi Ke Da Xue Xue Bao. 2023;43(8):1371–8.
25. Zhang M, Zhang Y, Jiao X, Lai L, Qian Y, et al. Identification and validation of immune related core transcription factors GTF2I in NAFLD[J]. PeerJ. 2022;10:e13735.
26. Sarahan KA, Fisler JS, Warden CH. Four out of eight genes in a mouse chromosome 7 congenic donor region are candidate obesity genes[J]. Physiol Genomics. 2011;43(18):1049–55.
27. Chen RX, Chen X, Xia LP, Zhang JX, Pan ZZ, et al. N(6)-methyladenosine modification of circNSUN2 facilitates cytoplasmic export and stabilizes HMGA2 to promote colorectal liver metastasis[J]. Nat Commun. 2019;10(1):4695.
28. Guo M, Yan R, Ji Q, Yao H, Sun M, et al. IFN regulatory Factor-1 induced macrophage pyroptosis by modulating m6A modification of circ_0029589

in patients with acute coronary syndrome[J]. Int Immunopharmacol. 2020;86:106800.
29. Chen YG, Chen R, Ahmad S, Verma R, Kasturi SP, et al. N6-Methyladenosine modification controls circular RNA Immunity[J]. Mol Cell. 2019;76(1):96–e109109.
30. Di Timoteo G, Dattilo D, Centrón-Broco A, Colantoni A, Guarnacci M, et al. Modulation of circrna metabolism by m(6)A Modification[J]. Cell Rep. 2020;31(6):107641.
31. Liu Y, Chen K, Shou Y, Li S, Wang J, et al. CircRARS synergises with IGF2BP3 to regulate RNA methylation recognition to promote tumour progression in renal cell carcinoma[J]. Clin Transl Med. 2023;13(12):e1512.
32. Wang D, Guan H, Xia Y. YTHDC1 maintains trophoblasts function by promoting degradation of m6A-modified circMPP1[J]. Biochem Pharmacol. 2023;210:115456.

Publisher's note